전력전자학술대회 논문집 2005. 7. 4 ~ 7. 7

AC-PDP의 광효율 향상을 위한 고주파 구동회로에 관한 연구

최성욱, 한상규, 문건우
한국과학기술원

A Study on High Frequency Sustaining Driver for Improving Luminance Efficiency of AC-PDP

Seong-Wook Choi, Sang-Kyoo Han and Gun-Woo Moon
Korea Advanced Institute of Science and Technology (KAIST)

ABSTRACT

Plasma display panel (PDP) has a serious thermal problem, because the luminance efficiency of the conventional PDP is about 1.5 lm/W and it is less than 3~5 lm/W of cathode ray tube (CRT). Thus there is a need for improving the luminance efficiency of the PDP. There are several approaches to improve the luminance efficiency of the PDP and we adopt the driving PDP at high frequency range from 400 kHz up to over 700 kHz. Since a PDP is regarded as an equivalent inherent capacitance, many types of sustaining drivers have been proposed and widely used to recover the energy stored in the PDP. However, these circuits have some drawbacks for driving PDP at high frequency range. In this paper, we investigate the effect of the parasitic components of PDP itself and driver when the reactive energy of panel is recovered. Various drivers are classified and evaluated whether it is suitable for high frequency driver, and finally current-fed type with dc input voltage biased is proposed. This driver overcomes the effect of parasitic component in panel and driver and fully achieves ZVS of all full-bridge switches and reduces the transition time of the panel polarity.

1. Introduction

The recent interest in flat panel display devices has made an alternating current (AC) PDP become a promising candidate for the conventional CRT display, because the PDP is praised for its large screen size, wide viewing angle, thinness, and high contrast[1]. However, PDP has serious heat problem, because the energy conversion efficiency is very low. It is reported that the luminance efficiency of PDP is 1.5 lm/W and it is less than 3~5 lm/W of CRT. There are several approaches to improve the luminance efficiency of PDP. The first method is changing the cell structure to spread out more phosphor in the cell and the second is increasing the Xenon ratio of the discharge gas mixture to obtain more ultraviolet rays (UV). Another method is driving the PDP at the higher frequency than usual[2]. The operation of the PDP can be divided into three periods such as resetting, addressing, and sustaining periods. Actually, since most of the light emission occurs during sustaining period, abovementioned high frequency driving means increasing the frequency of sustaining pulse from conventional 200 kHz up to over 700 kHz. Among them, we adopt driving the PDP at high frequency range to improve the luminance efficiency.

However, there is a serious problem accompanied by increasing the frequency of sustaining pulse. Since the sustaining electrodes of the PDP are covered with dielectric and MgO layer, a PDP can be regarded as an equivalent inherent capacitance C_P. Therefore, a considerable energy of $2C_PV_S^2$ for each sustaining cycle is dissipated in the non-ideal resistance of circuits and PDP during charging or discharging interval[3]. Also the sustaining driver which has a well-known full-bridge configuration with four sustain switches suffers from the large capacitive displacement current, which can give rise to an electromagnetic interference noise (EMI). To relieve these problems, many types of sustaining drivers, which reduce the capacitive displacement current and heating problem of switching devices by adopting the LC resonant technique, have been proposed[3]-[12]. However, these circuits have many serious drawbacks to drive the PDP at the high frequency.

In this paper, hitherto developed various energy recovery sustaining drivers are reviewed and compared to find out the most suitable PDP driver for the high frequency driving. Firstly, we investigate the effect of the parasitic components of the PDP and driving circuit when the energy recovery function of the sustaining driver is performed. Secondly, various energy recovery sustaining drivers presented in [3]-[12] are classified according to the voltage waveform across the PDP and current waveform through the energy recovery inductor and each sustaining driver is evaluated whether it is suitable for the high frequency driver. And It is tested to validate the proposed high frequency sustaining driver on 42-in panel and the experimental results are presented.

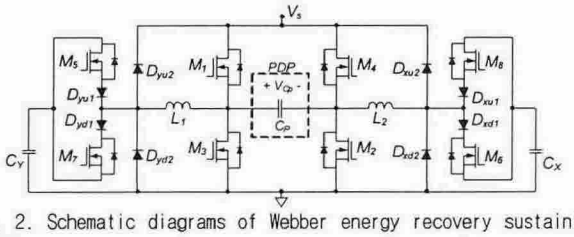

Fig. 2. Schematic diagrams of Webber energy recovery sustaining driver

2. Effect of parasitic component

Fig. 1 shows the Webber energy recovery sustaining driver, which features a high efficiency and good circuit flexibility to cope with various driving method[3]. Although this driver is widely used in the digital display industry, it has several serious problems when operated at high frequency range. To explain the effect of parasitic

components, it is assumed that the Webber's driver is operated at a high frequency range.

2.1 Effect of parasitic resistance

This driver has a severe problem that the reactive energy stored in the PDP cannot be fully recovered and the ZVS operation of all power switches cannot be obtained under the existence of the parasitic resistance. Fig. 2 shows its equivalent circuit and key waveforms considering the parasitic resistance during the energy recovery transient.

The current through the panel I_{Cp} and the voltage across the PDP V_{Cp} are obtained as

$$I_{Cp}(t)=\frac{1}{\omega L_{ERC}}\left(\frac{V_S}{2}-V_{on}\right)e^{-\frac{t}{\tau}}\sin(\omega t) \tag{1}$$

$$V_{Cp}(t)=\left(\frac{V_S}{2}-V_{on}\right)\left\{1-e^{-\frac{t}{\tau}}\left(\cos(\omega t)+\frac{1}{\omega\tau}\sin(\omega t)\right)\right\} \tag{2}$$

where V_S=input sustaining voltage, $\tau=2L_{ERC}$ / R_{ESR}, R_{ESR}=parasitic resistance of the driver, V_{ON} =forward voltage drop of the diode, and $\omega=[1/\{L_{ERC}(2C_{oss}+C_p)\}-1/\tau^2]^{0.5}$. Fig. 3 shows the theoretical voltage waveforms and power losses as a function of the equivalent series resistance (ESR). From these results, the sustaining driver suffers from the heat problem due to the hard switching operation of sustain switches, which becomes more and more serious when increasing the frequency of sustaining pulse.

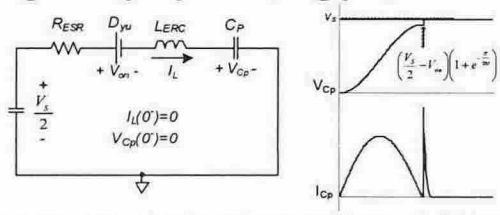

Fig. 2. Equivalent circuit and key waveforms of Webber driver considering parasitic resistance

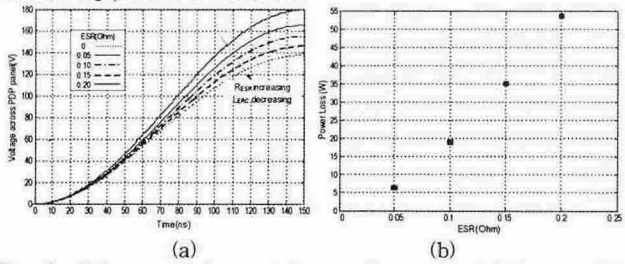

(a) (b)

Fig. 3. Voltage waveforms and power losses caused by parasitic resistance when rising time = 150 ns, switching frequency = 700 kHz(a) Voltage waveforms across the PDP (b) Power losses

2.2 Effect of parasitic inductance

It is very difficult to obtain the exact inductance for the energy recovery in a practical implementation, which is because the required inductance at high frequency range is much smaller than the parasitic inductance of the driver board and connection cable between the PDP and driver. Especially, in case that the energy stored in the parasitic inductance is large enough to flow its current through the PDP to the opposite direction of the energy recovery current, this parasitic inductance disturbs the energy recovery action.

To figure out the parasitic inductance of the driver board and the PDP, the voltage waveforms across the switch M_3 is measured at the operating frequency 200 kHz as shown in Fig. 4. As shown in this figure, the sub-oscillation is observed in the falling period of the sustaining pulse, which is because of the resonance between the parasitic inductance and output capacitance of sustain switches. From this waveform, this parasitic inductance is roughly obtained as

$$L_{ESL}=\left(\frac{T_{osc}}{2\pi}\right)^2\cdot\frac{1}{2\times2\times C_{OSS}}\simeq 63nH \tag{3}$$

where the switch output capacitor C_{OSS}=1nF is a known value and one resonant cycle of the sub-oscill ation T_{OSC}=100ns is a measured value.

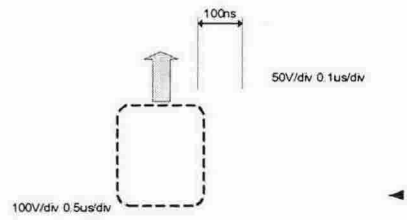

Fig. 4. Voltage waveforms across switch, M_3

To explain the effect of the parasitic inductance in recovering the panel energy, the Webber driver operating at the switching frequency 700 kHz for a 42-in PDP (C_P=80nF) is considered. If it is assumed that the rising/falling time of the panel voltage is 150 ns, respectively, and switch output capacitor C_{OSS} given as 1nF, the energy recovery inductor can be determined as follows:

$$L_{ERC}=\left(\frac{T_{rise}}{\pi}\right)^2\cdot\frac{1}{C_p+2\times2\times C_{oss}}\simeq 27nH \tag{4}$$

where T_{rise} is rising time of the panel voltage. Equation (4) shows that the required energy recovery inductance (i.e. L_{ERC}=27nH) is much smaller than the parasitic inductance (i.e. L_{ESL}=63nH). These facts say that the complete energy recovery operation of the panel energy satisfying as short period as 150 sec rising/falling time is impossible under the existence of the parasitic inductance.

Moreover this parasitic inductance hinders the driver from the energy recovery operation when parasitic inductance has enough energy to flow its current to the opposite direction of the energy recovery current. The parasitic inductance can have the initial value due to the following reasons.

The gas discharge current flows through the panel and parasitic inductance when the voltage across panel reaches breakdown point which visible light occurs at. Then, the resonance between the panel capacitor and parasitic inductor of the driver and PDP begins immediately after the light emission comes to an end. At the next transition period of the panel polarity, the energy recovery operation at the switching frequency 200 kHz is successfully performed, which is because the abovementioned resonance is completely eliminated before the driver recovers the panel energy. However, if operating the Webber driver at the switching frequency over 200 kHz, the energy recovery function can not be guaranteed by the resonance as shown in Fig. 5a. Also, the amplitude of this resonant current is directly proportional to the amplitude of discharge current or, in other word, the area of the light emitted from the PDP as shown in Fig. 5b. Fig. 6 shows the equivalent circuit and key waveform of Webber driver considering the parasitic inductance during the energy recovery transient. The current in the panel, I_{Cp}, and the voltage across the panel, V_{Cp}, are obtained as

$$I_{Cp}(t)=\frac{V_S/2-V_{on}}{Z_O}\sin(\omega t)+\frac{L_{ESL}}{L_{ERC}+L_{ESL}}I_d\cos(\omega t) \tag{6}$$

$$V_{Cp}(t)=V_S-\left(\frac{V_S}{2}-V_{on}\right)\left(1-\cos(\omega t)\right)-\frac{I_d}{\omega C_P}\frac{L_{ESL}}{L_{ERC}+L_{ESL}}\sin(\omega t) \tag{7}$$

where I_d represents initial current through the parasitic inductance when energy recovery function is achieved after the resonance between this inductance and inherent capacitance of panel, $Zo=[(L_{ERC}+L_{ESL})/C_p]^{0.5}$, L_{ESL}=parasitic inductance of the driver and PDP itself, and $\omega=1/[((L_{ERC}+L_{ESL})/C_p]^{0.5}$. Fig. 7 shows the theoretical waveforms and power losses according to the initial current of the parasitic inductance. Although there are no resistive components in equivalent circuit of driver except for the reactive components, the parasitic inductance and the energy stored in this inductance prevent the energy recovery function within the desired transition period. Especially, this problem is more serious when the direction of initial current in this inductance is against the current direction of the recovery inductor as shown in Fig. 7b.

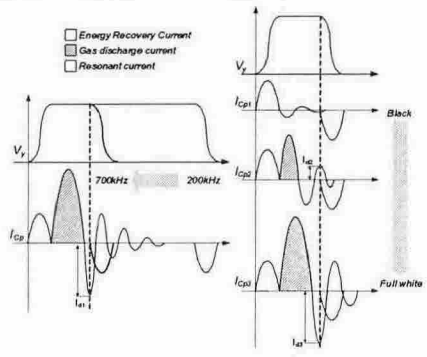

a. b.

Fig. 5. Effect of resonance between parasitic inductance and panel capacitance. a. when increasing frequency of sustaining pulse b. when increasing amplitude of discharge current

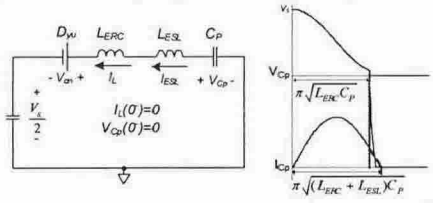

Fig. 6. Equivalent circuit and key waveforms of Webber driver considering parasitic inductance

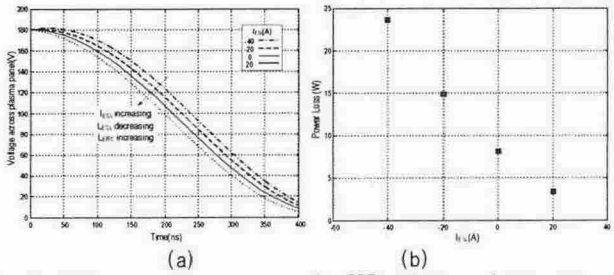

(a) (b)

Fig. 7. Voltage waveforms across the PDP and power losses caused by the parasitic inductance when rising time = 400 ns and switching frequency = 700 kHz (a) Voltage waveforms across PDP (b) Power losses

3. Evaluation of sustaining drivers

As described in section 2, Webber sustaining driver widely used in commercial product is not suitable for the high frequency driver because of the parasitic resistance and inductance on the driver and PDP itself. Therefore, to compensate the effect of parasitic components, it is necessary to develop a high frequency sustaining driver with the ZVS operation.

The desired features of the high frequency sustaining driver can be summarized as follows.

a) The energy recovery function must be achieved within the transition time below 200ns, which is essential to ensure the stable gas discharge and light waveform by making the effective pulse width of the sustaining waveform as long as possible.

b) The sustaining driver has to simultaneously recover the reactive energy of both side of the panel to reduce the transition time of the panel polarity.

c) The sustaining driver operated at high frequency should provide the PDP with more energy to compensate power loss due to parasitic resistance of driver and PDP itself. Since the power loss caused by the incomplete panel energy recovery is usually larger than the loss by the parasitic resistance, it is very important to ensure the complete energy recovery operation.

d) For the effective energy recovery action, the sustaining driver must have larger energy recovery inductance than the parasitic one as stated in equation (7).

e) Even though the sustaining driver provides more energy to overcome effect of parasitic components, the power consumption in it should be minimized to improve the luminance efficiency of AC-PDP.

The various sustaining drivers can be classified into three types according to the voltage waveform across the PDP and again, into five types according to the current waveform through the energy recovery inductor as shown in Fig. 8. In view of features mentioned above, each type of sustaining driver is evaluated whether it is suitable for high frequency driver.

First, we consider the voltage waveform across PDP to find out the proper sustaining driver at high frequency range. The multi-level types of sustaining drivers proposed in [5], [6] can not satisfy the required transition time because the energy recovery inductor of these drivers for desired rising and falling time must be much smaller than parasitic inductance and it is very difficult to obtain exact inductance of the energy recovery function in a practical implementation. Also, the three-level types of sustaining drivers proposed in [4], [7], [8] are not suitable for high frequency driver by the same reason multi-level types of the drivers have. Since the two-level types of sustaining drivers proposed in [3] and [9]-[14] can change the polarity of PDP at once, there is a possibility open to these drivers for high frequency driving.

Secondly, the two-level types of sustaining drivers are classified according to the shape of current waveform in the energy recovery inductor as shown in Fig. 8b. Although the continuous conduction current-fed types of two-level drivers proposed in [3], [9] have some desired features of high frequency sustaining driver, these drivers can not be directly applied to whole AC-PDP driver to display a image and have the severe problem that energy recovery efficiency of this driver is very low due to conduction loss of freewheeling current in the energy recovery inductor. Also, since the resonant type of two-level driver proposed in [10] can not fully recover the reactive energy of panel even at the absence of the parasitic inductance, this driver is not suitable for high frequency driver. And, the current-fed type drivers presented in [11], [12] have no bias voltage when the energy recovery function is achieved. Therefore, even though the energy recovery inductor of this driver has initial energy, this inductor is too small to guarantee fully recovering the reactive energy of panel at high frequency range.

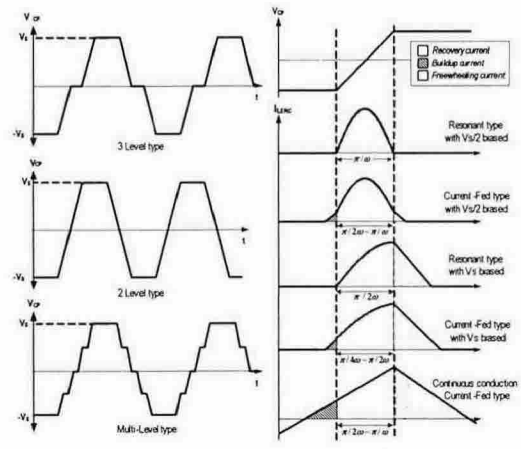

a. b.

Fig. 8. Classification of energy recovery sustaining driver. a. Accordingto voltage waveform across PDP b. According to current waveform in energy recovery inductor

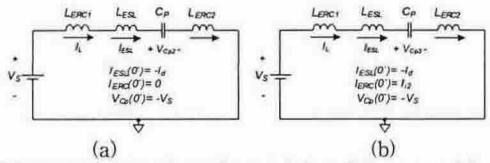

(a) (b)

Fig. 9. Equivalent circuits of sustaining driver considering the resonance between parasitic inductance and panel capacitance (a) resonant type with V_S biased (b) current-fed type with V_S biased

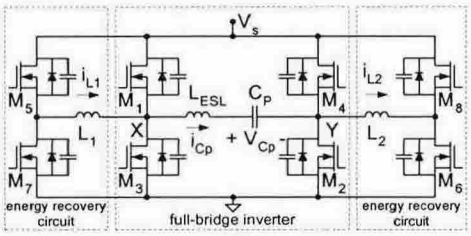

(a)

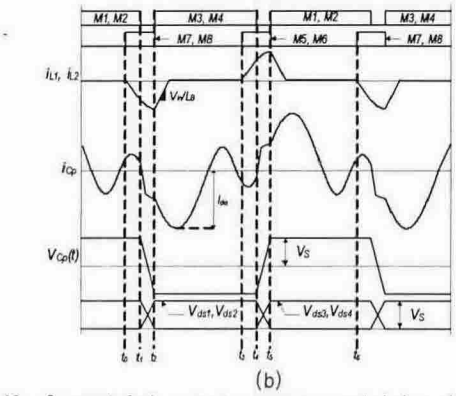

(b)

Fig. 10. Current-fed energy recovery sustaining driver with VS biased (a) Schematic diagram (b) Key waveform

The resonant type with V_S biased[13] and current-fed type with V_S biased[14] of two-level sustaining driver can be adopted to high frequency driver, but current-fed type with V_S biased shows the best capability to recover the reactive energy of panel during the desired transition time regardless of the parasitic components of driver and PDP itself. Fig. 9 shows the equivalent circuits of these sustaining drivers when reactive energy of panel is recovered. The voltages across the panel capacitance of each sustaining driver are obtained as

$$V_{Cp1}(t) = V_S\left(1-2\cos(\omega t)\right) - \frac{1}{\omega C_P}\frac{L_{ESL}}{L+L_{ESL}} I_d \sin(\omega t) \tag{8}$$

$$V_{Cp2}(t) = V_S\left(1-2\cos(\omega t)\right) + \frac{1}{\omega C_P}\left(\frac{LI_i - L_{ESL}I_d}{L+L_{ESL}}\right)\sin(\omega t) \tag{9}$$

where V_{Cp1} = voltage across PDP of resonant type driver with V_S biased, V_{Cp2} = voltage across PDP of current-fed type driver with V_S biased, $L = L_{ERC1} + L_{ERC2}$,$\omega = 1/[((L+L_{ESL})/C_p]^{0.5}$, and I_i represents the initial current in the energy recovery inductor to make this inductor act as a current source. As stated in (8) and (9), the initial current in parasitic inductance, I_d, directly affects the operation of the resonant type driver with V_S biased, but current-fed type driver with V_S biased ensures the energy recovery action even under the resonance of the parasitic component since the initial current I_i in energy recovery inductor compensates the initial current of the parasitic inductance. Therefore, this driver operated in current-fed with V_S biased overcomes the resonance of parasitic component in panel and driver board and fully achieves the ZVS of all full-bridge switches and reduce the transition time of the panel polarity, which is desirable for high frequency driving.

4. Operation of high frequency driver

Fig. 10 shows the circuit diagram and its key waveforms of the chosen high frequency sustaining driver. For the convenience of the analysis, it is only considered the effect of parasitic inductor except for parasitic resistor, which is because the energy recovery function of this driver can be fully achieved even under the existence of the parasitic resistance.

One cycle period of the chosen circuit is divided into two half cycles, $t_0 \sim t_3$ and $t_3 \sim t_6$. Because the operation principles of two half cycles are symmetric, only the first half cycle is explained. Before t_0, the voltage V_{Cp} across C_P is maintained to V_S with M_1 and M_2 conducting and panel current, I_{Cp}, is in resonance due to parasitic inductance and panel capacitance.

Mode 1($t_0 \sim t_1$): When M_7 and M_8 are turned on at t_0, mode 1 begins. The input voltage V_S is applied to L_1 and L_2 with M_1, M_2, M_7, and M_8 conducting. Thus, I_{L1} and I_{L2} increase linearly with the slope of V_S/L as $I_{L1}(t) = I_{L2}(t) = V_S(t-t_0)/L$, where it is assumed that the values of L_1 and L_2 are equal to L. I_{Cp} goes on with resonance.

Mode 2($t_1 \sim t_2$): When M_1 and M_2 are turned off at t_1, mode 2 begins. With the initial conditions of $I_{L1}(t_1) = I_{L2}(t_1) = V_S(t_1-t_0)/L$ and $V_{Cp}(t)=V_S$, I_{L1} and I_{L2} start to charge the PDP, but parasitic inductance disturbs this operation as follows:

$$I_{Cp}(t) = \frac{2V_S}{Z_O}\sin(\omega(t-t_1)) + \frac{LI_L(t_1) - L_{ESL}I_{Cp}(t_1)}{L+L_{ESL}}\cos(\omega(t-t_1)) \tag{10}$$

$$V_{Cp}(t) = V_S\left(1-2\cos(\omega(t-t_1))\right) + \frac{1}{\omega C_P}\left(\frac{LI_L(t_1) - L_{ESL}I_{Cp}(t_1)}{L+L_{ESL}}\right)\sin(\omega(t-t_1)) \tag{11}$$

where I_{Cp} = current through the PDP, V_{Cp} = voltage across the PDP of current-fed type driver with V_S biased, $L=L_1+L_2$, $\omega = 1/[((L+L_{ESL})/C_p]^{0.5}$. Because this driver injects PDP panel with the amount of energy proportional to $(LI_L(t_1) - L_{ESL}I_{Cp}(t_1))$ regardless of the panel resonant current as shown in Fig. 11, the abrupt charging and discharging operations of C_P are avoided and the voltage across C_P is decreased toward $-V_S$.

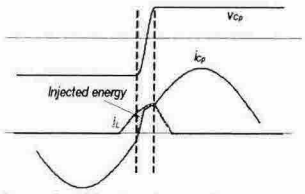

Fig. 11. Compensation of effect of panel resonance by current-fed type driver with VS biased

Mode 3(t_2~t_3): When V_{Cp} is clamped at $-V_S$, mode 3 begins. Since the voltage, V_{ds3} and V_{ds4}, across M_3 and M_4 are 0V, M_3 and M_4 can be turned on with ZVS. After M_7 and M_8 are turn off, the currents in energy recovery inductor begin to decrease linearly with the slope of V_S/L and the energy stored in the inductors is fed back to the input power source. After the gas discharge current I_{dis} reaches 0A, the resonance between parasitic inductance and panel capacitance occurs, and this resonance disturbs energy recovery function of this driver next time.

The circuit operation of t_3~t_6 is similar to that of t_0~t_3. Subsequently, the operation from t_0 to t_6 is repeated.

5. Experimental Results

To confirm the validity of the high frequency sustaining driver, a prototype PDP driver circuit has been designed for 42-in PDP with the following specifications: V_S=200~240V, switching frequency f_S =500~700kHz, ΔT=200ns, C_P=about 80nF, single scan, full white. Fig. 13 shows the sustaining voltage and energy recovery inductor current waveforms of the high frequency sustaining driver. As can be seen in Fig. 13, the current source built in the inductor completely charges the panel capacitor *Cp* to *Vs* or *-Vs* regardless of parasitic components. Fig. 12 shows that the measured luminance efficiency of PDP is about 2.6 lm/W in the frequency range from 500 kHz to 700 kHz.

6. Conclusion

In this paper, we investigate effect of parasitic components of PDP itself and driver when energy recovery function of sustaining driver is achieved, and the various energy recovery sustaining drivers are examined to find proper driver operated at high frequency range. The drivers are classified and evaluated whether it is suitable for high frequency driver, and the desired features of high frequency driver are suggested. Considering all necessary aspects for high frequency driver, finally current-fed type with dc input voltage biased is chosen. This driver overcomes the effect of the parasitic components in panel and driver and fully achieves zero voltage switching of all full-bridge switches and reduces the transition time of the panel polarity. It is tested to validate the high frequency sustaining driver on 42-in panel and the experimental results are presented according to increasing switching frequency of sustaining pulse in a range from 200 kHz to 700 kHz. With the proposed sustaining driver with 700 kHz switching frequency, the luminance efficiency is increased about 2.6 lm/W.

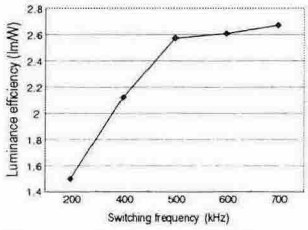

Fig. 12. Measured luminance efficiency of PDP

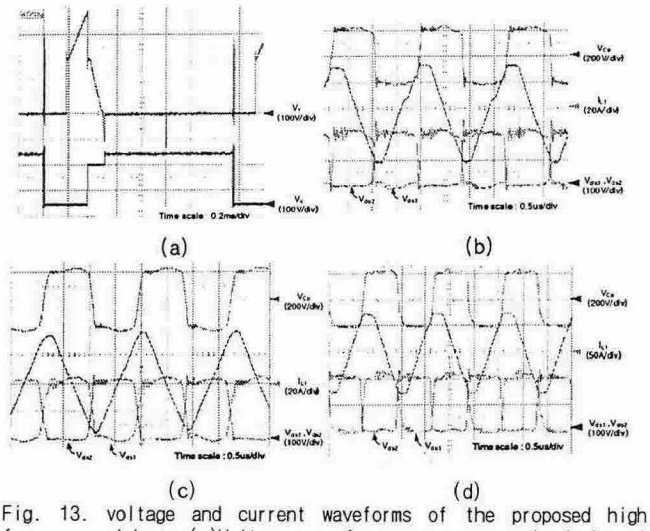

Fig. 13. voltage and current waveforms of the proposed high frequency driver (a)Voltage waveforms across panel during 1 subfield (b)At 500kHz (c)At 600kHz (d)At 700kHz

Reference

[1] A. Sobel, "Plasma displays," IEEE Trans. Plasma Sci., vol. 19, pp. 1032 - 1047, Dec. 1991.

[2] J.H. Choi, et al. "Space charge effect for sustaining discharge in coplanar AC-PDP," IDW'02, pp873 - 876, 2002

[3] S. Y. Lin, C. L. Chen, and K. M. Lee, "Novel regenerative sustain driver for plasma display panel," in Proc. IEEE PESC'98, pp 1739 - 1743, Fukuoka, Japan, 1998.

[4] L. F. Webber and K. W. Warren, "Power efficient sustain drivers and address drivers for plasma panel," U.S. Patent 4 866 349, Sept. 1989.

[5] C. W. Roh, H. J. Kim, S. H. Lee, and M. J. Youn, "Multilevel voltage wave-shaping display driver for AC plasma display panel application," IEEE J. Solid-State Circ., Vol.38, No.6, pp.935 - 947, Jun. 2003.

[6] C. W. Roh, "Novel plasma display driver with low voltage / current device stresses," IEEE Trans. Con. Electron., Vol. 49, No. 4, pp.1360 - 1366,November 2003.

[7] D. Y. Lee, J. H. Yang, and B. H. Cho, "Novel energy-recovery circuit for plasma display panel using regenerative transformer," in Proc. IEEE PESC'03, Vol.2, pp.656 - 659, June 2003.

[8] H. van der Broeck, M. Wendt, "Alternative sustain driver concepts for plasma display panels," in Proc. IEEE PESC'04, Vol. 4, pp.2672 - 2677, June 2004.

[9] S. K. Han, G. W. Moon, and M. J. Youn, "Current-fed energy-recovery circuit for plasma display panel," Electronics Letters, Vol. 39,14,pp 1035 - 1036, July 2003.

[10] M. Ohba and Y. Sano, "Energy recovery driver for a dot matrix AC plasma panel with a parallel resonant circuit allowing power reduction,"U.S. Patent 5 670 974, Sept. 1997.

[11] C. C. Liu, H. B. Hsu, S. T. Lo, and C. L. Chen, "An energy-recovery sustaining driver with discharge current compensation for AC plasma display panel," IEEE Trans. Ind. Electron., Vol. 48, No. 2, pp.344 - 351, Apr. 2001.

[12] J. Y. Lee, J. S. Kim, N. S. Jung, and B. H. Cho, "The current injection method for AC plasma display panel (PDP) sustainer," IEEE Trans. Ind. Electron., Vol. 51, No. 3, pp.615 - 624, Jun. 2004.

[13] S. K. Han, G. W. Moon, and M. J. Youn, "A resonant energy-recovery circuit for plasma display panel employing gas-discharge current compensation method," IEEE Trans. Power Electron., Vol. 20, No.1 ,pp. 209 - 217, Jan. 2005.

[14] S. K. Han, G. W. Moon, and M. J. Youn, "A novel current-fed energy recovery sustaining driver for plasma display panel (PDP)," in Proc. IEEE IECON '03, Vol. 2 ,pp. 1976 - 1980, Nov. 2003.